MSW MANAGEMENT -Multidisciplinary, Scientific Work and Management Journal
ISSN: 1053-7899
Vol. 36 Issue 1, 2026, Pages 5734-5739

Multifunctional Performance of Bio-Based Polyurethane Composites Reinforced with Graphene Oxide Nanoparticles

Muhammad Abdurrahman Munir[1], Fitria Rahmawati[2], Ahlam Inayatullah[3], Sofian Ibrahim[4]

[1] Faculty of Resource Science and Technology, Chemistry Department, Universiti Malaysia Sarawak, Kota Samarahan, Malaysia.
[2] Faculty of Mathematics and Natural Sciences, Research Group of Solid Chemistry and Catalysis, Chemistry Department, Sebelas Maret University, Surakarta, Indonesia.
[3] Food Technology Study Program, Chemical Engineering Department, Sriwijaya State Polytechnic, Palembang, Indonesia.
[4] Malaysian Nuclear Agency, Kajang, Malaysia.
Email: [1]mmabdurrahman@unimas.my, [2]fitria@mipa.uns.ac.id, [3]ahlam.inayatullah@polsri.ac.id [4]sofian_ibrahim@nm.gov.my
Orchid Id number: [1]0000-0001-6129-6202, [2]0000-0002-3145-9063, 0000-0002-0708-0854 [3]0000-0002-1898-6432
Corresponding Author*: Muhammad Abdurrahman Munir.

ABSTRACT:*The development and multifaceted efficacy of bio-based polyurethane composites reinforced with graphene oxide (GO) nanoparticles are described in this study. Polyol produced from palm kernel oil combined with methylene diphenyl diisocyanate to fabricate polyurethane (PU), which provides a sustainable basis for cutting-edge functional materials. To improve the PU properties, GO was used at various concentrations (1, 2, 5, and 10%) using a sonication-assisted solution casting method. Fourier Transform Infrared Spectroscopy (FTIR) was applied to verify the urethane linkages and the disappearance of isocyanate structure, and it demonstrated satisfactory molecular compatibility by revealing hydrogen-bonding interactions between the GO functional groups and PU chains. At the higher loadings of GO, the Field Emission Scanning Electron Microscopy (FESEM) exhibited uniform GO dispersion throughout the matrix with little agglomeration. TGA and DSC were employed to study the thermal properties of PU and PU/GO, and they demonstrated a definite improvement in thermal stability, where PU/GO showed a delayed degradation initiation, and improved char production at higher levels of GO. A stable matrix structure and limited polymer chain mobility were further investigated by DSC. The conductivity of PU/GO was confirmed by Electrochemical Impedance Spectroscopy (EIS) to study the synergistic electron-ion transport, showing a significant decrease in bulk and charge-transfer resistances with increasing GO levels. The addition of GO improved the insulating bio-based PU into an electroconductive and thermally stable composite that could be considered for flexible electronics, protective coatings, and bioelectronic devices, where the PU/GO materials offer a high-performing and sustainable alternative.*

KEYWORDS:**Bio-based, characterization, electrical conductivity, graphene, polyurethane**

1) Introduction

The transition from petroleum-based polymers to bio-based substitutes has accelerated owing to the increased environmental consciousness and the pressing demand for sustainable products. Researchers are studying renewable resources as feedstocks for polymer synthesis owing to the depletion of fossil fuel reserves and the negative ecological consequences of petrochemical operations [1,2]. Among them, vegetable oils including castor, soybean, and palm kernel oils (PKOs) are particularly appealing owing to their hydroxyl functionality, their availability, and biodegradability. Polyol is one of the imperative materials to fabricate the polyurethanes (Pus) could be fabricated chemically from these oils. Flexible foams, adhesives, coatings, and elastomers with lower carbon footprints and superior performance adaptability could be fabricated using the bio-based Pus [3,4].

Despite their usefulness, the PUs are generally known to have low electrical conductivity, mechanical strength and thermal stability compared to the petrochemical-based equivalents. In order to improve the PUs characteristics, many studies reported the addition of nanoscale fillers, including nanoclay, gold, carbon nanotubes, and graphene. [5-7]. Because of its distinct two-dimensional structure, high aspect ratio, and abundance of oxygen-containing functional groups that foster robust interfacial interactions with polar polymer chains, graphene oxide (GO) draws attention from numerous researchers [8,9].

Nevertheless, attaining homogeneous GO dispersion within polymer matrix is quite challenging in the fabrication of PU/GO composites. Aggregation usually occurs due to the strong van der Waals forces and π–π stacking interactions among GO, which may lower the predicted reinforcing impact and interfacial bonding efficacy. Liang et al., described the synthesis of PU/GO nanocomposite with increasing the tensile strength and improved the thermal stability, however, the higher GO levels, the agglomeration occurred that causing a mechanical degradation [10]. Similarly, another study reported that the addition of GO improved the conductivity and thermal resistance of polymer, but led to the embrittlement and diminished the PU film flexibility [11].Consequently, the successful incorporation of GO into PU continues to be a critical issue that require more attention in terms of the synthesis and dispersion approach. A considerable number of studies have focused on modifying the mobility and uniform dispersion of FO in polymer matrices. Guanjung et al. (2025) reported, by limiting the chain mobility and having a stronger hydrogen bonding, the application of GO into polymer increased the tensile modulus and glass transition temperature [12]. Similar to this, another study reported the improvement in electrical conductivity of PU/GO composites owing to the percolation conductive networks at modestly [13]. Another study also reported the improvement of PU/GO in its thermomechanical stability and char yield. These outcomes were attributed to the barrier qualities and heat dissipation capacity of GO sheets [14-16]. However, these studies neglected the optimization of three parameters at once and instead focused on the thermal, mechanical, or electrical improvements.The aforementioned literature makes it clear that, despite significant advancements in PU/GO properties, having multifaceted enhancement such as mechanical robustness, thermal stability and satisfactory conductivity remains a crucial gap. The majority of several reports presented the increased thermal stability may reduce the mechanical performance or having a satisfactory conductivity may decrease the flexibility of polymer [17-22]. Moreover, the combination of GO into PU generated from palm kernel oil (PKO), has not received much attention. It is yet unclear how GO dispersion affects the microstructure-property connection in these kinds of green composites.Bio-based polyurethane/graphene oxide (PU/GO) composites produced from polyol generated from palm kernel oil and MDI are synthesized and characterized in this study. It investigates the effects of various GO loadings (1–10 wt%) on the mechanical, electrical, thermal, and structural characteristics. For uniform GO dispersion and excellent interaction with the PU matrix, a solution casting technique aided by sonication is employed. The work demonstrates that interfacial adhesion is improved without chemical modification via non-covalent interactions, particularly hydrogen bonding between GO and PU. The article explains how dispersion and matrix-filler bonding enhance multifunctional performance by adjusting GO content, facilitating the creation of high-performance, sustainable polymer nanocomposites.

2) Methods and Methodology

(a) **Chemicals and Reagents.**Munir et al. (2023) method was applied to produce PU with few adjustments [23]. The the palm kernel oil (PKO) and 4,4-diphenylmethane diisocyanate (MDI) were purchased from PT Chemie Mitra Indonesia. Graphene oxide (GO) and N, N-dimethylformamide (DMF) were purchased from Sigma Aldrich. All chemicals used in the studies were analytical grade to ensure precision and dependability. Analytical-grade chemicals were employed throughout the study to guarantee precise and reliable outcomes. Deionized water kept at 4 °C was employed for all solution preparation to ensure uniformity and minimize any potential deterioration.

(b) **PU/GO production.**GO (1, 2, 5, and 10 wt%) was prepared by dissolving in DMF within an Erlenmeyer flask. The sonication process was performed to get a homogenous solution at 60 °C under continuous magnetic stirring. The procedure was repeated until a dark, ink-like solution was obtained, showing the complete dispersion of GO. Afterward, the GO was added in the 5 mL (PU) and stirring slowly until a uniform blend was obtained. The mixture then was cast into the specific mold and waited for 6 hours in a vacuum oven at 50 °C.

(c) **Morphological, Thermal, and Conductivity Analysis of PU/GO composites.**Prior to analysis, PU/GO films were conditioned at ambient conditions for 1 day. **Surface Morphology**: The morphological features of the PU/GO composites were investigated using a Field-Emission Scanning Electron Microscope (FESEM, model JSM-6510 LA), coupled with Energy Dispersive X-ray (EDX) spectroscopy to assess elemental composition and verify the uniform dispersion of GO within the polymer matrix. **Thermal Analysis**: **Thermogravimetric Analysis (TGA)**: Thermal stability was investigated using a PerkinElmer Pyris TGA system. Approximately 10 mg analyzed from 40 °C to 800 °C at a heating rate of 25 °C·min^{-1} under N_2 flow of 50 mL·min^{-1}. **Differential Scanning Calorimetry (DSC)**: Thermal transitions behavior was examined using a PerkinElmer Pyris DSC. Approximately 10 mg was sealed in aluminum pans and heated from 25 °C to 150 °C at 20 ° C·min^{-1}, held for 3 min, then cooled to –100 °C. A second heating from –100 °C to 200 °C was performed to determine the glass transition temperature (T*g*) from the heat-flow inflection point. **Structural analysis: FTIR Analysis**: FTIR was employed to analyze the chemical bonding within the PU/GO composites.

MSW MANAGEMENT -Multidisciplinary, Scientific Work and Management Journal
ISSN: 1053-7899
Vol. 36 Issue 1, 2026, Pages 5734-5739

Spectra were collected using a Thermo Scientific Nicolet iS10 system with a Diamond Attenuated Total Reflectance (DATR) accessory. Key functional groups, such as –NH, –CH, –NCO, and –C=O, were evaluated to confirm structural features and polymer-filler interactions. **Conductivity: Electrochemical Impedance Spectroscopy (EIS):** Electrical properties were evaluated using an Electrochemical Workstation at Sebelas Maret University, Indonesia. Measurements employed a three-electro configuration, with the PU/GO as the working electrode (WE), platinum wire as the counter electrode (CE), and the reference electrode (RE) was Ag/AgCl. Analysis was conducted at open-circuit potential (OCP) over frequencies ranging from 10 MHz to 10 kHz with a 10 mV signal amplitude. Impedance data were analyzed using ZView software to investigate the resistance and capacitance characteristics.

3) Results and Discussion. FTIR was employed to validate the PU/GO fabrication and also to verify the interactions between GO and PU (Figure 1). Table 1 presents the several absorption peaks and corresponding function groups for MDI, palm kernel oil as polyol, PU and PU/GO composites.

The polyol showed a wide absorption band around 3338 cm^{-1}, arising from the overlapping O-H stretching of terminal hydroxyl groups and the N-H stretching associated with urethane linkages in the resulting PU network. This feature remained visible in PU and PU/GO spectra, showing the retention of -OH and -NH that implying the presence of hydrogen-bonding interactions along the polymer backbone. Comparable broad of -OH and -NH signals have been identified in other bio-based PU materials, where inter- and intra-molecular hydrogen bonding enhances flexibility and mechanical resilience [24].

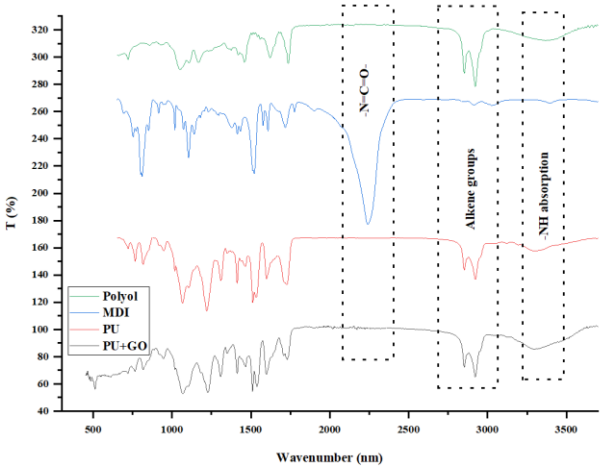

Figure 1. FTIR spectral profile of PU/GO, PU, MDI, and Polyol. Two prominent peaks at 2922 cm^{-1} and 2853 cm^{-1} are attributed to the asymmetric and symmetric stretching of aliphatic -CH_2 groups. These signals appear in the spectra of the polyol as well as the PU and PU/GO, reflecting the aliphatic nature derived from the PKO-based polyol. Their persistence indicates that the soft segments of the PU remain flexible even after the addition of GO, a behavior commonly reported for PU systems synthesized from vegetable oils [25]. For MDI spectrum, a sharp peak at 2241 cm^{-1} linked to the -N=C=O, known as isocyanate group, stretching vibration of free isocyanate groups. This peak is absent in PU and PU/GO, indicating that this group completely reacted with the polyol's hydroxyl groups to form urethane linkages. The disappearance of the -N=C=O band confirms complete polymerization and the formation of a stable PU [26,27]. The urethane group (C=O), linked to the carbonyl group found at 1729 cm^{-1}. In the PU/GO, this wavenumber becomes slightly more intense and shifts to a lower wavenumber compared to the PU itself, suggesting that the carbonyl groups linked on the hydrogen bonding with the oxygen-containing functionalities on GO, including carboxyl and hydroxyl groups. This shift strongly supports the presence of interfacial interactions between the PU and GO. Similar trends have been reported in other PUs and epoxy systems composited with GO, where such non-covalent interactions improve interfacial stability and facilitate efficient stress transfer [28-30].Absorption bands identified at 1599 cm^{-1}, 946 cm^{-1}, 817 cm^{-1}, and 758 cm^{-1} linked to the aromatic (C=C) stretching and out-of-plane C-H bending modes. These features originate from the aromatic rings of MDI incorporated into the PU backbone. Their consistent presence in all PU-based samples indicated that the hard segment domains, which is MDI, is the vital to the rigidity and thermal resistance of PU, and the properties remain intact despite the GO addition. Similar aromatic signatures have been reported in PU composites prepared from aromatic diisocyanate, supporting the retention of structural stability within the hard-segment [31-32].Subtle variations in peak intensity were also noted as the GO content increased. The slight broadening and enhancement of the wavenumber at 3338 cm^{-1}, together with a slight shift of the carbonyl peak at 1729 cm^{-1}, point to stronger hydrogen-bonding interactions and decreased chain mobility in the GO composite. These spectral changes suggest improved interfacial compatibility between the polar GO and the urethane groups, a trend commonly associated with the enhanced thermal and mechanical properties in the PU/GO [33-34].

There are sixteen significant peaks were verified, and each of them linked to the functional groups present in the polyol, MDI, PU, and PU/GO (Table 1). The collective data of FTIR spectrums reveal the complete reaction of PU as bio-based and showing that GO is incorporated through non-covalent hydrogen bonding rather than chemical grafting. These connections are anticipated to contribute significantly to the improved multifaceted performance of the composites, especially in terms of thermal stability, mechanical reinforcement, and electrical behavior.

Table 1. Analysis of Infrared Spectral Characteristics of PU-GO, PU, MDI, and Polyol

No.	Peak wavenumber (cm^{-1})	Functional group interpretation	Vibration mode	Intensity	Wavenumber range reference (cm^{-1})	Dominant compound
1	3338	N–H (urethane or amine) or O–H (polyol)	Stretching	Broad, Strong	3700-3200	PU, PU/GO, Polyol
2	2922	Aliphatic alkane (C-H)	Stretching	Strong	3000-2850	PU, PU/GO, Polyol
3	2853	Aliphatic alkane (C-H)	Stretching	Strong	3000-2850	PU, PU/GO, Polyol
4	2241	Isocyanate (-N=C=O)	Asymmetric stretching	Strong	2276 – 2240	MDI
5	1729	C=O in urethane (-COO)	Stretching	Strong	1750-1730	PU, PU/GO, Polyol
6	1599	Aromatic C=C	Stretching	Medium-weak	1600-1475	PU, PU/GO
7	1539	Amide N-H (-NHCOO- in urethane linkage)	Bending	Medium-Strong	1640-1550	PU, PU/GO
8	1466	Alkane C-H	Bending	Medium	1450-1375	PU, PU/GO, Polyol
9	1413	CH_2 scissoring or O–H bending	Scissoring or bending	Medium	1440–1380	PU, PU/GO, MDI
10	1350	Amine C-N	Stretching	Medium-strong	1350-1000	PU, PU/GO
11	1308	C-O (Ester) in urethane linkage	Stretching	Strong	1300-1000	PU, PU/GO
12	1228	C-O (Ester) in urethane linkage	Stretching	Strong	1300-1000	PU, PU/GO
13	1068	C-O (Ester) in urethane linkage	Stretching	Strong	1300-1000	PU, PU/GO, Polyol
14	946	Aromatic C-H	Out-of-plane bending	Strong	1000-650	PU/GO, PU (weaker)
15	817	Aromatic C-H	Out-of-plane bending	Strong	1000-650	PU/GO, PU (weaker), MDI
16	758	Aromatic C-H	Out-of-plane bending	Strong	1000-650	PU/GO, PU (weaker), MDI

MSW MANAGEMENT -Multidisciplinary, Scientific Work and Management Journal
ISSN: 1053-7899
Vol. 36 Issue 1, 2026, Pages 5734-5739

Field Emission Scanning Electron Microscopy (FESEM) was applied in this study to complement the FTIR outcomes and verify the complete incorporation of GO within the PU matrix, as shown in Figure 2a-d. Images captured at magnifications between 200× and 5000× reveal that the bare PU possesses a smooth and uniform surface with observable defects. This implies that the PU is being formed properly, and the hard and soft segments within PU are well aligned. Such smooth surface is commonly reported for bio-based PU materials derived from vegetable oils [35].
Furthermore, when the GO introduced to the PU, no cracks, phase-separated regions, or noticeable GO agglomerates were investigated, even at the highest concentrations (10%). These observations suggest that the GO nanosheets dispersed effectively throughout the polymer and were strongly embedded in the matrix. This behavior is consistent with the interfacial bonding interactions inferred from the FTIR spectrums. The lack of void or clusters further exhibits satisfactory compatibility between PU and GO, likely facilitated by the oxygenated groups on GO that enhance interactions with urethane linkages [36-37].
At higher magnifications, the PU/GO samples exhibited subtle surface texturing and fine wrinkled patterns that are not exist in the bare PU. These features correspond to the presence of uniformly dispersed GO nanosheets and reflect their layered nature within the polymer. The slight roughening of the surface is linked with improved load transfer and mechanical reinforcement, as the addition of GO can more effectively anchor and dissipate stress. Similar morphological trends have been reported in other PU/GO composites, where a higher concentration of GO introduces micro-scale surface features without influencing the structural integrity of the coating [38-39].

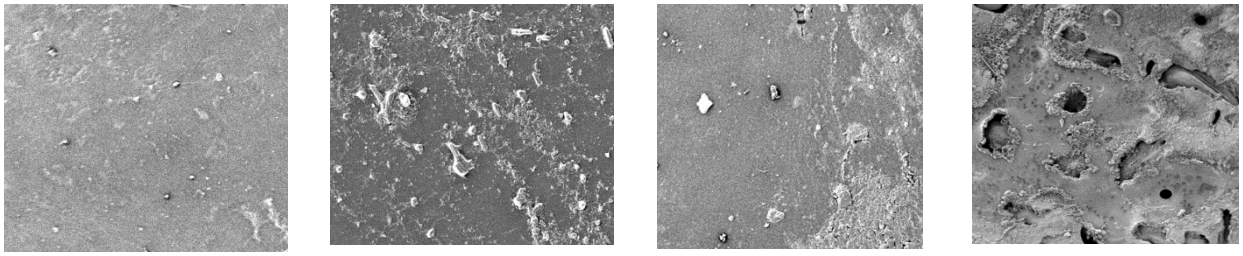

Figure 2. Surface morphology of PU and PU/GO captured via FESEM at 200× and 5000× magnifications (images a & b for PU; c & d for PU/GO).

No sign of phase irregularities or particle clustering were identified, implying that the sonication approach completely obtained a homogenous form between PU and GO. Achieving this level of dispersion is imperative because it strengthens filler-matrix connectivity, which in turn contributes to improved mechanical performance, enhanced thermal resistance, and the development of conductive pathways within the composite [40]. The FESEM outcomes therefore support the FTIR data, indicating that GO are evenly dispersed and strongly linked within the PU chains through non-covalent interactions. This close morphology-structure relationship is the key to the multifaceted improvements noted in the composites [41-42]. Furthermore, to investigate the GO effect in terms of the thermal stability, TGA and DSC were applied (Figure 3a-b). Together, these methods provide insights into degradation pathways, thermal transitions, and the impact of GO on the structural resilience of the polymer.
The TGA profiles for PU and PU/GO composites exhibited the multi-step decomposition pattern typically linked to the segmented PU systems. The onset of thermal degradation occurred near 20 °C for PU, corresponding to the breakdown of relatively labile urethane and urea linkages within the soft segment regions. This early degradation step in also reported in the flexible PU from vegetable oil-derived polyols, which contain ester and ether groups that are less thermally stable compared to the aromatic hard segments [43]. The major degradation occurred between 350 °C and 400 °C, corresponding to the cleavage of urethane bonds and the disintegration of the hard segment structures, including aromatic units derived from MDI. This phase of weight loss arises from chain scission, depolymerization, and the release of volatile compound including CO_2 and amines, reflecting the breakdown of carbamate linkages [44].
Whereas, the onset of degradation shifted to 250 °C, owing to the presence of GO in the PU system, indicating improved thermal resistance. This stabilization is linked to the thermal conductivity and barrier characteristics of GO, which slow the transfer of heat and volatile products during decomposition. The well-distributed GO create tortuous pathways that hinder the escape of degradation gases and provide additional thermal shielding to the polymer matrix [45]. Although the GO levels varied from 1 to 10%, the initial degradation temperature remained unchanged, indicating that low to moderate GO contents primarily improve the degradation kinetics rather than the fundamental degradation mechanism. Once a uniform dispersion of GO is obtained, increasing the filler concentration offers limited additional protection, likely owing to the decreased effectiveness of excess particles or the onset of minor agglomeration [46].

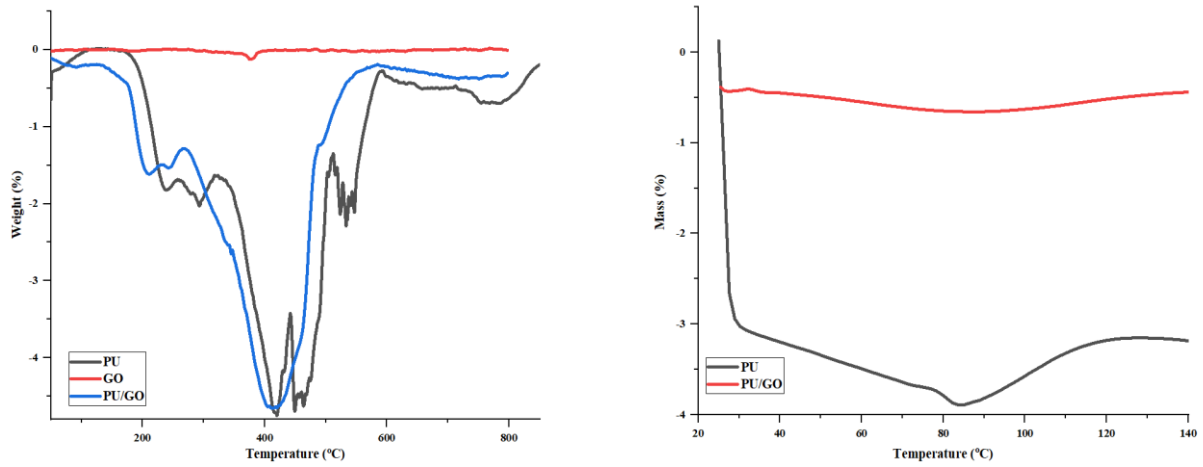

Figure 3. (a) DTG curves illustrating the thermal decomposition of PU, PU/GO, and GO, and (b) DSC analysis of PU and PU/GO

The principal decomposition phase in the PU/GO appeared at slightly higher temperatures, around 370-430 °C, compared to the PU, indicating an improvement in thermal robustness. This shift alteration is linked to the strong interfacial interactions between the polymer chains and the GO, especially hydrogen bonding involving GO's oxygenated functionalities and the urethane groups, which increases the energy barrier for bond cleavage. Furthermore, the rigid, plate-like structure of GO inhibits polymer chain movement, further slowing the breakdown process [47]. PU/GO showed comparable two-step decomposition patterns with identical residues at 630 °C. This implies that while GO promotes the formation of a stable carbon-rich protective layer, it does not alter the overall degradation pathway of

MSW MANAGEMENT -Multidisciplinary, Scientific Work and Management Journal
ISSN: 1053-7899
Vol. 36 Issue 1, 2026, Pages 5734-5739

the PU. The higher char content reinforces the concept that GO contributes to a thermally insulating barrier that shields the polymer from oxidative attack during heating [48]. For comparison, GO itself, may exhibit negligible mass loss during this process, demonstrating its intrinsic thermal resilience and supporting its role as an effective stabilizing composite.

Another information of thermal properties was acquired from the DSC (Figure 3b). The PU showed a relatively broad glass transition (T*g*) around 30 °C and 60 °C, indicating the soft-segment domains derived from the PKO-based polyol. A modest endothermic feature at 85 °C was also recorded, representing relaxation phenomena between the soft and hard segments, and the transition from a rigid to a more rubber-like phase [49]. Furthermore, for the PU/GO, the DSC profiles were unchanged in terms of the transition temperatures, regardless of GO levels. Nevertheless, the enthalpic features were less pronounced, indicating the GO limits segmental mobility and contributes to a more uniform phase arrangement within the composite. These effects are consistent with strong interfacial interactions and the confining influence of GO's layered structure, both of which reduce microphase separation between the polymer segments [50].

The absence of new thermal, either exothermic or endothermic, demonstrates the GO does not trigger additional crosslinking or induce instability within the matrix. Moreover, its presence appears to improve thermal consistency and resistance to softening, an imperative factor for maintaining mechanical and electrical performance across varying operating temperatures. Similar studies have been reported in the previous studies on PU/GO applications [51].

In order to evaluate the electrochemical behavior and conductivity of the PU/GO, the EIS was employed. Measurements were applied in phosphate-buffer solution (PBS, 0.01 mol·L^{-1}, pH 7.2). The impedance profiles were interpreted using Randles equivalent circuit, a general model for describing charge-transfer resistance (R*ct*), double-layer capacitance (Cdl), and diffusion contributions at the coating-electrolyte interface [52].

Each sample exhibit the typical EIS response of a semicircle in the high-frequency area followed by a linear diffusion-controlled tail at lower frequencies (Figure 4). The semicircular portion corresponds to the charge-transfer process, while the-low frequency segment relates to the Warburg diffusion. The appearance of a well-defined semicircle across all coatings shows the formation of a stable double-layer interface and confirms that the PU-based films remain electrochemically intact [53].

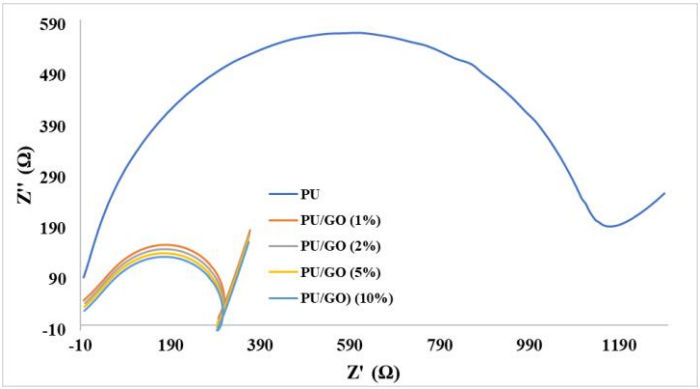

Figure 4. Electrochemical impedance profiles of PU and PU/GO coatings with different GO loadings.

The Nyquist plot for the PU shows a wide semi-circle, which is typical of a highly insulating material with substantial bulk resistance (Rb). This behavior is predicted owing to the polymer's aliphatic and aromatic components do not contain delocalized π-electron that capable to support the charge movement. As a result, the material responds largely in a capacitive manner, consistent with the many studies of insulation PU [54]. Nevertheless, the addition of GO affected the size of semi-circle, demonstrating a steady reduction in overall impedance and a clear improvement in conductivity. This enhancement is attributed to the formation of new conductive routes as GO link to the polymer chains. Owing to their large aspect ratio and planar geometry, even small levels of GO may form effective electron-hopping and tunnelling pathways, contributing to lower Rb and R*ct* [51].

Increasing the GO levels from 1 to 10% leads to a decline in charge-transfer resistance, reflected by the shrinking semi-circle size. It shows a direct link between GO levels and the number of conductive composites within matrix. At lower levels (1-2 %), GO are mainly well-separated yet still provide modest improvements in charge mobility. Once the percolation threshold is reached (around 5%), these sheets begin to form continuous electron-conducting bridges throughout the polymer, producing a more significant enhancement in electrical response [55]. Nevertheless, the improvement becomes less substantial at 10%. At this point, some of GO sheets start to cluster, decreasing their available surface area and adding interfacial resistance between overlapping layers. This behavior mirrors findings from other polymer-GO composites, where very high levels of composites cause partial agglomeration, limiting conductivity and even may decrease the mechanical strength of polymer [14].

At low frequencies, all samples display a linear tail liked to Warburg impedance, which arises from ion transport at the polymer-electrolyte interface. The gradual decrease in this slope with higher GO concentrations suggests that ions can move more freely within the modified polymer. This enhancement is supported by the presence of polar oxygen-functional groups on GO, which increase the surface polarity of the composite and improve ion accessibility and charge exchange at the interface [56]. Moreover, to improve ionic movement, the GO facilitates better electron-ion coupling, enabling faster charge transfer between the PU and the surrounding electrolyte. The combination of percolated electronic pathways and enhanced ionic mobility produced a satisfactory conduction mechanism, elaborating the consistent drop in bulk resistance and at the same time improving the electrochemical properties of PU/GO composites.

4) Conclusion

The effective manufacturing of bio-based polyurethane (PU) composites reinforced with graphene oxide (GO) is demonstrated in this study. Strong interfacial contacts were fabricated by combining the GO into the PU made from palm kernel oil (PKO)-based polyol, which enhanced dispersion and stress transmission. Satisfactory affinity of GO and the PU was confirmed by the composites' homogeneous surface with no aggregation. Because of GO's barrier effect and chain mobility limitation, thermal testing revealed greater stability, delayed degradation, and enhanced char accumulation. Electrochemical investigation showed the formation of conductive channels and decreased resistance. All things considered, these PU/GO composites offer a sustainable path toward long-lasting, thermally stable, and semiconductive coatings and devices.

5) Acknowledgement

We thank Muhammad Abdurrahman Munir, Fitria Rahmawati, Imam Shofid Alaid and Ahlam Inayatullah for their contributions to this work. The authors would like to acknowledge and express their gratitude to Universiti Malaysia Sarawak (UNIMAS) via the International Matching Grant funds (INT/F07/UNS/86787/2025) and the Faculty of Resource Science and Technology (FRST) for providing research facilities and other forms of assistance.

6) Funding Statement

The authors did not receive financing for the development of this research.

7) Data Availability

MSW MANAGEMENT -Multidisciplinary, Scientific Work and Management Journal
ISSN: 1053-7899
Vol. 36 Issue 1, 2026, Pages 5734-5739

No new data were created or analyzed in this study. Data sharing is not applicable to this article.

8) Conflict of Interest

The authors declare that there is no conflict of interest.

9) References

[1] Sharma BK, Jha A, Bhalani D, Pillai SA, Pal S, et al. Advancements in bio-resource-based polymers and composites: Sustainable alternatives to non-biodegradable plastics for a greener future: A review. Current Green Chemistry. 2025; 12.
[2] Saxena P, Shukla P. A green approach to sustainability: biodegradable polymers in environmental and energy applications. ECS Journal of Solid State Science and Technology. 2025; 14(6): 063005.
[3] Zhang Y, Dong H, Yang W, Lu H, Wei C, et al. Recent progress on bio-based polyurethanes: Synthesis, structure and cutting-edge applications. Materials Today Communications. 2025; 45: 112279.
[4] Yao L, Baharum A, Yu LJ, Yan Z, Badri KH. A vegetable-oil-based polyurethane coating for controlled nutrient release: A review. Coatings. 2025; 15(6): 665.
[5] Wang J, Dong X, Qiu H, Liu Z, Kang Y, et al. Bioinspired structure with hierarchical hydrogen bonding and metal coordination for enhanced properties of biobased polyurethane applied in artificial ligaments. Chemistry of Materials. 2025; 37(4): 1609-1620.
[6] Wang J, Liu Z, Qiu H, Wang C, Dong X, et al. A robust bio-based polyurethane employed as surgical suture with help to promote skin wound healing. Biomaterials Advances. 2025; 166: 214048.
[7] Jaisingh A, Halloran MW, Rajput BS, Burkart MD. Tailoring High Hardness and Rigidity in Biodegradable Thermoplastic Polyurethanes. ACS Applied Polymer Materials. 2024; 6(16): 9724-9734.
[8] Sinh LH, Luong ND, Seppala J. Enhanced mechanical and thermal properties of polyurethane/functionalised graphene oxide composites by in situ polymerization. Plastics, Rubber and Composites. 2019; 48(10): 466-476.
[9] Albozahid M, Naji HZ, Alobad ZK, Wychowaniec JK, Saiani A. Synthesis and characterization of hard copolymer polyurethane/functionalized graphene nanocomposites: Investigation of morphology, thermal stability, and rheological properties. Journal of Applied Polymer Science. 2022; 139(45): e53118.
[10] Liang G, Yao F, Qi Y, Gong R, Li R, et al. Improvement of mechanical properties and solvent resistance of polyurethane coating by chemical grafting of graphene oxide. Polymers. 2023; 15(4): 882.
[11] Owji E, Ostovari F, Keshavarz A. Electro-thermal properties and characterization of the flexible polyurethane-graphene nanocomposite films. Physica Scripta. 2022; 97(10): 105704.
[12] Liu G, Liu Y, Zhang M, Zhao D, Liu P, Wang L, Li L, Yan M. Covalently bonded graphene oxide–carbon nanotube hybrid nanofillers for achieving high-performance polyamide 6 composites with superior mechanical properties and thermal conductivity. Nanoscale. 2025; 31(17): 18127-18142.
[13] Sadavar SV, Padalkar NS, Shinde RB, Patil AS, Patil UM, et al. graphene oxide as an efficient hybridization matrix for exploring electrochemical activity of two-dimensional cobalt-chromium-layered double hydroxide-based nanohybrids. ACS Applied Energy Materials. 2022; 5(2): 2083-2095.
[14] Pramodkumar B, Budhe S. The effect of graphene oxide on thermal, electrical, and mechanical properties of carbon/epoxy composites: Towards multifunctional composite material. Polymer Composites. 2024; 45(7): 6374-6384.
[15] Heydari SF, Shahgholi M, Karimipour A, Salehi M, Galehdari SA. The effects of graphene oxide nanoparticles on the mechanical and thermal properties of polyurethane/polycaprolactone nanocomposites; a molecular dynamics approach. Results in Engineering. 2024; 24: 102933.
[16] Tian X, Sun Y, Xie H, Shi B, Zhing J, et al. Preparation of graphene oxide/ waterborne polyurethane via boric acid cross-linked dopamine enhanced barrier and mechanical properties. Frontiers in Materials. 2022; 9: 1046125.
[17] Zhang P, Xu P, Fan H, Sun Z, Wen J. Covalently functionalized graphene towards molecular-level dispersed waterborne polyurethane nanocomposite with balanced comprehensive performance. Applied Surface Science. 2019; 471: 595-606.
[18] Samanta PN, Majumdar D, Leszcynski J. Effects of graphene reinforcement on morphology, thermophysical, and mechanical properties of polyvinyl alcohol and polyacrylamide in condensed phases. Computational and Theoritical Chemistry. 2024; 1241: 114875.
[19] Xia J, Zhu Y, He Z, Wang F, Wu H. Superstrong noncovalent interface between melamine and graphene oxide. ACS Applied Materials and Interfaces. 2019; 11(18): 17068-17078.
[20] Chen X, Fu X, Chen Z, Zhai Z, Miu H, et al. Multifunctional polyimide for packaging and thermal management of electronics: Design, synthesis, molecular structure, and composite engineering. Nanomaterials. 2025; 15(15): 1148.
[21] Kim D. PEDOT: PSS-based high-performance thermoelectrics. 2024; 32(12): 1187-1198.
[22] Sharma A, Sharma S, Sharma M, Sharma V, Sharma S, et al. Polymeric frontiers in next-generation energy storage: bridging molecular design, multifunctionality, and device applications across batteries, supercapacitors, solid-state systems, and beyond. Polymers. 2025; 17(20): 2800.
[23] Munir MA, Jamal JA, Said MM, Ibrahim S, Ahmad MS. Polyurethane application to transform screen-printed electrode for rapid identification of histamine isolated from fish. Scientifica. 2023; 2023(1): 5444256.
[24] Zhang J, Zhang C, Song F, Shang Q, Hu Y, Jia P, Liu C, Hu L, Zhu G, Huang J, Zhou Y. Castor-oil-based, robust, self-healing, shape memory, and reprocessable polymers enabled by dynamic hindered urea bonds and hydrogen bonds. Chemical Engineering Journal. 2022; 429: 131848.
[25] Baishya J, Gogoi K, Maji TK. Sustainable nanocomposites based on modified vegetable oil and coconut fiber reinforced with functionalized multiwalled carbon nanotubes. Next Materials. 2026; 10: 101386.
[26] Khalid T, Naheed S, Rehman FU, Salman M. Advancing sustainable adhesive: potential use of recycled polyethylene terephthalate (PET) polyols for the synthesis of polyurethane hot melts adhesive. Journal of Saudi Chemical Society. 2025; 29(18).
[27] Vijayan JG, Chandrashekar A, Jineesh AG, Prabhu TN, Kalappa P. Polyurethane and its composites derived from bio-sources: Synthesis, characterization and adsorption studies. Polymers and Polymer Composites. 2022;30.
[28] Dewangan R, Asthana A, Singh AK, Carabineiro SAC. Control of surface functionalization of graphene-metal oxide polymer nanocomposites prepared by a hydrothermal method. Polymer Bulletin. 2021; 78(8): 4665-4683.
[29] Ghazi RA, Al-Mayalee KH, Al-Bermany E, Hashim FS, Albermany AKJ. Impact of polymer molecular weights and graphene nanosheets on fabricated PVA-PEG/GO nanocomposites: Morphology, sorption behavior and shielding application. AIMS Materials Science. 2022; 9(4): 584-603.
[30] Pasieczna-Patkowska S, Cichy M, Flieger J. Application of fourier transform infrared (ftir) spectroscopy in characterization of green synthesized nanoparticles. Molecules. 2025; 30(3): 684.
[31] Zaho X, Wang J, Li J, Yu Q. Kinetic modeling of thermal degradation of TDI/MDI-based flexible polyurethane foam under nitrogen and air atmospheres with shuffled complex evolution algorithm: Insights from TG-FTIR analysis. Journal of Analytical and Applied Pyrolysis. 2024; 177: 106279.
[32] Karimi AS, Khorasani SN, Masoomi M, Neisiany RE, Dinari M. Synthesis and properties of a shape memory–assisted self-healing supramolecular polyurethane coating based on quadrupole hydrogen bonding. Polymers for Advanced Technologies. 2024; 35(12): e6617.
[33] Marbun L, Zebua HLP, Faldo A, Nissa RC, Iasya YKAA, et al. Thermoplastic agar/pbat blending as the alternative substitution of polyethylene. Journal of Applied Polymer Science. 2025.
[34] Wu DD, Tan Y, Cao ZW, Han LJ, Zhang HL, et al. Preparation and characterization of maltodextrin-based polyurethane. Carbohydrate Polymer. 2018; 194: 236-244.
[35] Min-Hui P, Shu-Qi D, Guo-Yuan Z, Hong-Yan L, Li-Na L, et al. Preparation of palm oil-based degradable coating materials and the property study. Journal of Plant Nutrition and Fertilizers. 2023; 29(10): 1966-1976.

MSW MANAGEMENT -Multidisciplinary, Scientific Work and Management Journal
ISSN: 1053-7899
Vol. 36 Issue 1, 2026, Pages 5734-5739

[36] Jing Q, Liu W, Pan, Y, Silberschmidt VV, Li L, et al. Chemical functionalization of graphene oxide for improving mechanical and thermal properties of polyurethane composites. Materials and Design. 2015; 85: 808-814.
[37] Lan Y, Liu H, Cao X, Zhao S, Dai K, et al. Electrically conductive thermoplastic polyurethane/polypropylene nanocomposites with selectively distributed graphene. Polymer. 2016; 97: 11-19.
[38] Zhang N. Largely improved mechanical properties of polyurethane nanocomposites via in situ polymerization with low loading of graphene oxide. Journal of Macromolecular Science, Part B: Physics. 2022; 61(4-5): 571-583.
[39] Mo M, Zhao W, Chen Z, Yu Q, Zeng Z, et al. Excellent tribological and anti-corrosion performance of polyurethane composite coatings reinforced with functionalized graphene and graphene oxide nanosheets. RSC Advances. 2015; 5(70): 56486-56497.
[40] Navidfar A, Trabzon L. Recent advances in the multifunctional properties and applications of carbon nanotube/graphene hybrid polymer nanocomposites. Polymer Composites. 2025.
[41] Han X, Gao J, Chen Z, Tang X, Zhao Y, et al. Correlation between microstructure and properties of graphene oxide/waterborne polyurethane composites investigated by positron annihilation spectroscopy. RSC Advances. 2020; 10(54): 32436-32442.
[42] Wen Z, Zheng Y, Wang W, Li Y, Wang Z, et al. Mechanical properties and functionalization of graphene oxide-thermoplastic polyurethane polymer composites regulated by internal microstructure: From disorder arrangement to nacre-like laminated structure. Polymer Composites. 2024; 45(11): 9819-9830.
[43] Li JF, Ku XL, Li YD, Ran Y, Zeng JB. Biobased polyamides with polyethylene-like properties through catalyst-free polycondensation. ACS Sustainable Chemistry & Engineering. 2025; 13(33): 13492-13500.
[44] Belleghem LV, Dirix R, Silva RDO, Wery J, Sakellariou D, Velthoven NV, Vos DD. Recovery of polyol and aromatic amines from rigid polyurethane foams via ammonolysis. JACS Au. 2025; 5(7): 3444-3452.
[45] Yang Z, Wang Z, Li J, Ding S, Yi S. Effect of graphene oxide-based nanodielectric on electrical discharge machining performance of Ti-6Al-4 V. Langmuir. 2025; 41(33): 21981-21991.
[46] Li XL, Guo JG, Zhao ZN, Zhou LJ, Zhang XR. In-plane dynamic crushing and energy absorption of three-dimensional graphene. International Journal of Mechanical Sciences. 2025; 291-292: 110146.
[47] Wang Y, Dong X, Wang Y, Hu Z, Chen Y, Yu J, Zhu M. Enhanced mechanical properties of aramid fiber/epoxy composites through reinforcing interfacial adhesion based on strong hydrogen bonding interactions. Composites Science and Technology. 2025; 262: 111057.
[48] Nguyen TA, Nguyen VH. Advanced bio-based pva composite films reinforced with bacterial cellulose and graphene oxide: Enhanced mechanical, thermal, flame-retardant, and uv-blocking properties. Trends in Sciences. 2025; 22(11): 10357.
[49] Chen Y, Tian F, Yao J, Li L, Cui Y, Yang H, Chen Z, Sun G, Shuttleworth PS, Yue H. Biobased polyurethane adhesives derived from vegetable oil and rosin for flexible packaging applications. ACS Applied Polymer Materials. 2024; 6(11): 6469-6481.
[50] Guo T, Li Z, Chen Y, Xu Q, Wang J, Jin L. Study on the performance and mechanism of graphene oxide / polyurethane composite modified asphalt. Scientific Reports. 2025; 15: 2482.
[51] Zhou L, Li Y, Wang S, Zhao J, Wu Z, Hao X, Barzagli F, Zhang R, Li C. Layer-by-layer assembled graphene oxide-enhanced poly(vinyl alcohol)/polyurethane coatings on stainless-steel substrate as hydrogen barriers. Materials Chemistry and Physics. 2025; 346: 131396.
[52] Silva RD, Catunda LGDS, Buoro RM. Multiple comparisons of acetylene black–based rigid composite electrodes: comprehensive evaluation of chemical properties and electrochemical sensing potentialities. Journal of Solid State Electrochemistry. 2024; 28: 3999-4013.
[53] Qader IN, Muhammed AW, Rasul HH, Mohammed SS, Hamid DA, et al. Enhancing ion transport in MC/dextran-based polymer electrolytes: Effect of glycerol plasticization on nanocomposite properties. Electrochimica Acta. 2025; 538: 146976.
[54] Munir MA, Rahmawati F, Jamal JA, et al. Fabrication and characterization of new bio-based electrode polyurethane: diverse conducting materials impacts such as graphene oxide, gold, and carbon nanotube. Green Chemistry Letters and Reviews. 2024; 17(1): 2355235.
[55] Chen F, Wang L, Li Guo R, et al. Self-limiting selective phase separation of graphene oxide and polymer composite solution. Nanoscale. 2025; 5(17): 2793-2799.
[56] Yin Y, Tan S, Zhang D, Shiery RC, et al. Distinct ion transport behavior between graphene oxide and UV-irradiated reduced graphene oxide membranes. Chemical Engineering Journal. 2024; 493: 152304.